

Eruption Histories of Zao and Azuma Volcanoes and Their Magma Feeding Systems for Recent Activities

Masao Ban^{1)*}, Yoshinori Takebe¹⁾, Tatsuya Adachi¹⁾, Ruriko Matsui¹⁾ and Yuki Nishi¹⁾

¹⁾Earth and Environmental Sciences, Faculty of Science, Yamagata University

Abstract

Since the 2011 Tohoku-Oki earthquake on March 11, 2011, several dormant volcanoes have shown signs of activity. In particular, many phenomena that are precursors to eruptions have been detected at Zao and Azuma volcanoes, which are located near the hypocenter of this earthquake. Eruption histories and current conditions of these volcanoes are reviewed, and the states of present sub-volcanic systems are considered on the basis of petrologic features of recent magmatic eruption products coupled with geophysical data.

Both volcanoes have eruption histories of approximately 1 million years. At Zao, the first stage, ~1 Ma, is characterized by sub-aqueous eruptions of basaltic magma followed in stages by small to medium-sized andesitic stratovolcanoes building at ~0.5–0.04 Ma. The youngest stage, ~35 ka to the present, is characterized by explosive eruptions of basaltic andesite to andesitic magma. This stage is further divided into three phases: ~35 to 13 ka, ~9 to 4 ka, and ~2 ka to the present. During the youngest phase, the Goshikidake cone-building phase, many historical eruptions were recorded; the youngest eruption from the present crater occurred in AD 1895. At Azuma, volcanic activity is divided into five stages: 1.2–0.8 Ma, 0.8–0.6 Ma, 0.6–0.4 Ma, 0.4–0.3 Ma, and less than 0.3 Ma. During each stage, small to medium-sized andesitic stratovolcanoes formed over the entire area of Azuma. The youngest activity began at about 7 ka in the eastern area. Five magmatic eruptions at ~6.7 ka, ~6.3 ka, ~5.9 to 4.8 ka, ~4.3 ka, and ~AD 1331 and seven phreatic eruption episodes have been recognized by tephrostratigraphic studies. Many historical eruptions have also been recorded; the youngest eruption from the present crater occurred in AD 1977.

Volcanic tremors were first detected at Zao in January 2013. Although such tremors were also recorded at Azuma, those with larger amplitudes have been detected since January 2010. The number of volcanic earthquakes increased beneath Zao in April 2015 and beneath Azuma in December 2014. At those times, volcanic tremors and deformation of the summit area were observed in both cases, which led to volcanic activity warnings. At both volcanoes, other precursory phenomena have been observed, including an increase in underground temperature revealed by total magnetic force surveys and an increase of geothermal activity. At Zao, the number of low-frequency earthquakes increased about one year before the first detection of volcanic tremors was reported.

Magmatic eruptions of <~35 ka of Zao and <~7 ka of Azuma volcanoes produced basaltic andesites to andesites, which were formed by the mixing of mafic and felsic magmas. The felsic magmas are andesitic at Zao and dacitic at Azuma, containing about 60% and 65.5% SiO₂, respectively. The temperature, pressure, and water content of these magmas are 955–970°C, 1.3–1.5 kb, and 1.7–1.8% H₂O; and 880–890°C, 0.8–1.2 kb, and 2.75–3.25% H₂O, respectively. The mafic magmas are basaltic in both cases, but that of Zao is slightly more differentiated than that of Azuma. In both cases, deeper mafic magmas infiltrated the shallower felsic magma chamber, which triggered the eruption.

The felsic chamber locations, at ~6 km at Zao and ~4 km at Azuma, are deeper than the present shallow earthquakes. The shallow earthquakes are related to hydrothermal fluid released from shallow felsic chambers that have been reactivated. The deep earthquakes occurred in areas with a high P-wave to S-wave velocity ratio (V_p/V_s) at depths of about 20–37 km below both volcanoes, where tomographic studies indicate melt. Therefore, the mafic magma probably originated from the melt.

Keywords: Zao volcano, Azuma volcano, eruption history, 2011 Tohoku-Oki earthquake, magma feeding system

* e-mail: ban@sci.kj.yamagata-u.ac.jp (1-4-12, Kojirakawamachi, Yamagata, Yamagata 990-8560, Japan)

1. Introduction

Since the 2011 Tohoku-Oki earthquake on March 11, 2011, several dormant volcanoes have shown signs of activity. In particular, many phenomena that are precursors to eruption, such as volcanic tremors, have been detected at Zao and Azuma volcanoes, which are located in the central part of the Quaternary volcanic front of northeast Japan and are near the hypocenter of the 2011 Tohoku-Oki earthquake (Fig. 1).

Understanding the magma feeding system beneath active volcanoes is fundamental for evaluating their unrest. For active volcanoes with present-day eruptions, such as Pu'u O'o at Kilauea and Mount Etna in Italy, petrologic monitoring of the magma feeding system in real-time is possible (Garcia *et al.*, 2000; Shamberger and Garcia, 2007; Nicotra and Viccaro, 2012). For active volcanoes with many historical records of eruptions, such as Colima in Mexico and Miyakejima in Japan, temporal variations in magma feeding systems over hundreds of years can be inferred (Savov *et al.*, 2008; Amma-Miyasaka and Nakagawa, 2003). While the eruption rates of these active volcanoes are usually high, the eruption rates of most volcanoes in northeast Japan are low. This limitation creates difficulties in collecting samples systematically from the eruption history and in

performing petrologic monitoring of the magma feeding system.

In the cases of Zao and Azuma volcanoes, exhaustive research has revealed much of their eruption histories, particularly recent activity. Petrologic studies have also been performed on recent eruption products. In the present study, we outline the eruption histories of Zao and Azuma volcanoes, as well as some precursory phenomena that have been detected recently. Moreover, we describe a petrologic model of the magma feeding systems beneath both volcanoes based on recent petrologic studies coupled with new data.

2. Eruption histories of Zao and Azuma volcanoes

2-1. Zao volcano

Zao volcano is situated in the central part of the volcanic front of northeast Japan (Fig. 1). Volcanic activity commenced at about 1 Ma (Takaoka, *et al.*, 1989) and has continued to the present. A simplified geological map of the summit area of Zao volcano based on Ban *et al.* (2015) is shown in Fig. 2.

Comprehensive geologic and petrologic studies of activity have been conducted by Tiba (1961), Oba and Konta (1989), and Sakayori (1991, 1992) among others. According to the most recent study by Ban *et al.* (2015), activity is divided into six stages. The first stage, ~1 Ma, is characterized by subaqueous eruptions of basaltic magma. In the second to fifth stages, small to medium-sized andesitic stratovolcanoes were formed, in which the location of the eruption center changes among stages. The eruption products are mainly lava flows and dome lavas in stages two to four and lavas and pyroclastic flows in stage five.

The youngest stage of Zao volcano, stage six, began at about 35 ka. At that time, the horseshoe-shaped Umanose caldera, which is 1.7 km in diameter, was formed in the summit area. Since then, numerous small to medium-sized eruptions ejecting basaltic andesite to andesitic magmas have occurred. This activity is subdivided into three phases that produced Kumanodake-Komakusadaira-Kattadake pyroclastic rocks at ~35 to 13 ka, Umanose agglutinate at ~9 to 4 ka, and Goshikidake pyroclastic rocks at ~2 ka to the present. A small cone, Goshikidake, formed in the inner part of Umanose caldera at <2 ka. This activity is characterized by explosive eruptions and subordinate lavas.

Crater Lake Okama lies in the western part of Goshikidake, and the pre-Okama crater is situated just

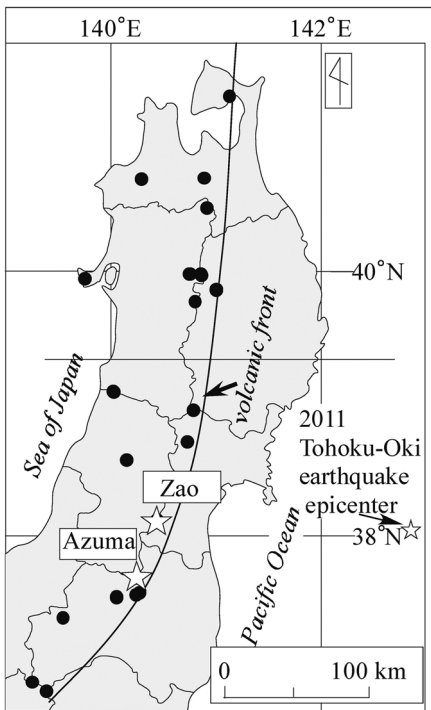
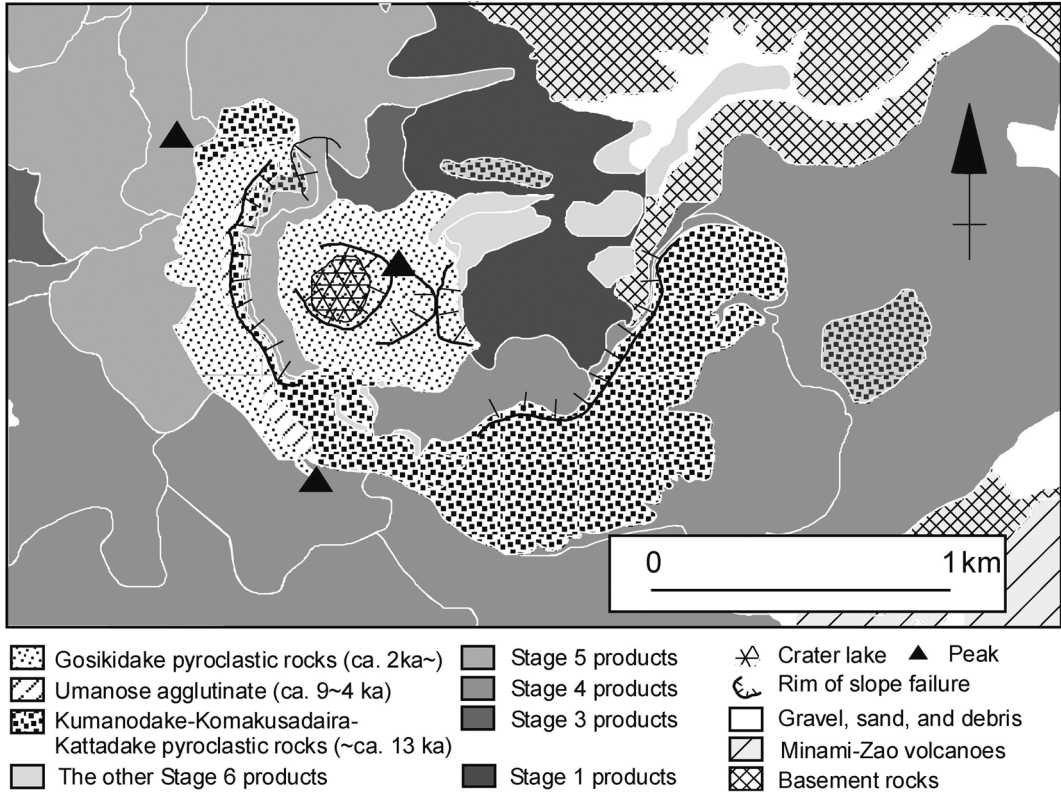


Fig. 1. Locality map of Zao and Azuma volcanoes. Filled circles represent Quaternary volcanoes.

Fig. 2. Geological map of summit area of Zao volcano after Ban *et al.* (2015).

southeast of Okama (Fig. 3a). Okama has been the eruption center since ~800 years ago. At least seven subsequent eruption episodes have been identified by tephrostratigraphic studies (Ban *et al.*, 2015), and many historical activities have also been recorded. Oikawa and Ban (2013) reported that the oldest credible record of an eruption is that occurring in AD 1230. Subsequent eruptions were recorded with a high degree of reliability in the mid-14th century and AD 1620–1625, 1641, 1668–1670, 1694–1697, 1794–1796, 1804, 1806, 1809, 1813, 1821–1822, 1831–1833, 1867, and 1894–1897.

The latest eruption episode in the Okama crater occurred from AD 1894 to 1897 (Kochibe, 1896); the sequence of this activity is summarized by Miura *et al.* (2012), Oikawa and Ban (2013), and Ban *et al.* (2015). The first eruption, a small-scale phreatic eruption, which occurred on July 3, 1894, was followed by small phreatic eruptions on February 15, February 19, and August 22, 1895. The climactic eruption, which occurred on September 27, 1895, was also phreatic, but included small amounts of juvenile materials (Ban, 2013). On the next day, another small phreatic eruption occurred, after which activity declined. Sketch maps of the climactic

eruption of September 27 and the fumarole occurring on October 6 are presented in Fig. 3b and c.

According to Ban *et al.* (2015), activity after AD 1894–1897 is summarized as follows. Precursory phenomena such as changes in the color of lake water were observed in AD 1918 and 1923. Although the phenomena intensified in AD 1939–1943, no eruption occurred in Okama. However, a very small-scale eruption occurred in the Maruyamazawa geothermal area about 1.5 km northeast of Okama. Afterward, an increase in volcanic fumarole activity in the Maruyamazawa geothermal area occurred in AD 1949. From AD 1968 to AD 1972, the same phenomena occurred with the formation of new hot springs at that location and similar phenomena in several areas other than the summit. Many earthquakes were detected in AD 1984, 1990, 1992, and 1995.

A stable hydrothermal system developed beneath the volcanic edifice at Zao. Numerous acidic hot springs and related fumaroles surround these spas, and their chemical compositions, resulting in sulfate and sulfate-chloride waters, are attributed to injections of volcanic gases derived from a cryptic magma body.

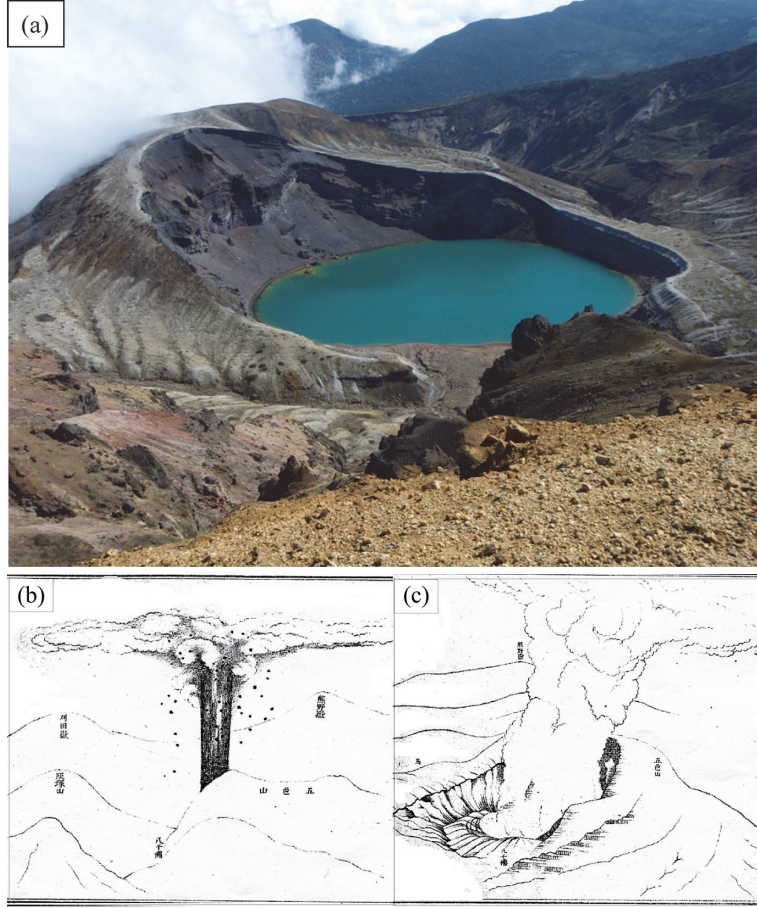


Fig. 3. (a) Aerial photograph of Goshikidake and Okama crater. (b) Sketch map of the climactic eruption on September 27, 1895. (c) Sketch map of the fumarole occurring on October 6, 1895. Figures (b) and (c) are from Kochibe (1896).

2-2. Azuma volcano

The eruption products of Azuma volcano are distributed across a wide area of about 25 km from east to west and about 15 km from south to north. Many small to medium-sized volcanic edifices comprise a volcano group (Fig. 4; Fujinawa and Kamoshida, 1990).

Azuma volcano also has a long eruption history, and its geological features have been outlined in previous studies (*e.g.*, Kawano *et al.*, 1961; Kuno, 1962; NEDO, 1991). Ban *et al.* (2013) divided volcanic activity into five stages of 1.2–0.8 Ma, 0.8–0.6 Ma, 0.6–0.4 Ma, 0.4–0.3 Ma, and < 0.3 Ma on the basis of K-Ar data presented by NEDO (1991) (Fig. 4). The main eruption products are andesitic lava flows, although lava domes or pyroclastic cones were formed in the summit area in the later part of each period. The eruption products were widely distributed over the entire area of Azuma volcano in every stage.

According to Yamamoto (2005), the youngest activity began at about 7 ka and occurred in numerous

craters formed in the Issaikyo area at the eastern part of Azuma. From northwest to southeast, these include Goshikinuma crater, Issaikyo crater, the Issaikyo-minami crater chain, Oana crater, the Tsubakurosawa crater chain, the Iwodaira-minami crater chain, Kofuji crater, and Okenuma crater (Fig. 5). Yamamoto (2005) recognized five magmatic eruption phases including Okenuma at ~6.7 ka, Goshikinuma at ~6.3 ka, Kofuji at ~5.9 to 4.8 ka, Issaikyo at ~4.3 ka, and Oana at ~AD 1331 and seven phreatic eruption phases referred to as Jododaira P1–P7 by tephrostratigraphic investigation. The Jododaira P1 phase is between Goshikinuma and Kofuji phases and from the Issaikyo-minami crater chain. The Jododaira P2–P6 phases are between the Issaikyo and Oana phases and from Issaikyo crater. An exception is P5–P6, in which the eruption centers were south or southwest of the Iwodaira-minami crater chain. The Jododaira P7 phase corresponds to the recorded eruption of AD 1711 from or near the Oana crater. A columnar section of a representative outcrop is shown in

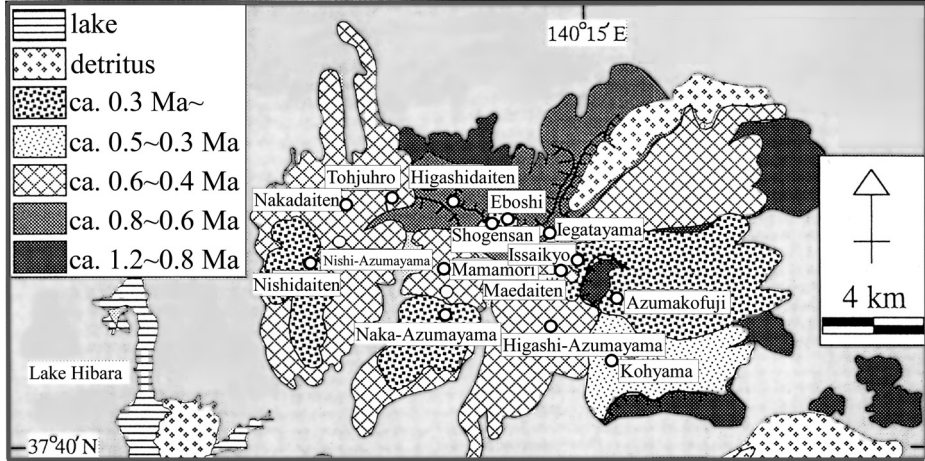


Fig. 4. Simplified geological map of Azuma volcano after Ban *et al.* (2013). Ages are estimated on the basis of NEDO (1991).

Fig. 5. We note that the eruption products of the five magmatic phases are named Okenuma, Goshikinuma, Kofuji, Issaikyo, and Oana units, respectively.

During each magmatic phase, pyroclastic materials were deposited around the crater, and sometimes formed a pyroclastic cone. In addition, single or multiple andesitic ash to lapilli layers were formed in the medial to distal area. In the Kofuji phase, lavas also swelled out. The tephra layers of the phreatic eruptions are composed of yellow- to white-colored ash.

The oldest recorded eruption occurred at about AD 1331 from the Oana crater and the Iwodaira-minami crater chain. Subsequently, many historic eruptions were recorded in written accounts (Geological Survey of Japan, 2016). Among these, the phreatic eruptions of AD 1711 and 1893–1895 were remarkable. The former occurred from or near the Oana crater, and the latter from the Tsubakurosawa craters. The latter eruptions began with a phreatic eruption on March 19, 1893, and continued intermittently until September 1895. Afterward, a volcanic plume was observed in AD 1914, and phreatic eruptions occurred in AD 1950, 1952, and 1977. The volcanic fumaroles around Oana and the Iwodaira area are still active (Fig. 6a, b). Since November 11, 2008, fumarole activity has intensified.

3. Outline of geophysical data from Zao and Azuma volcanoes following the 2011 Tohoku-Oki earthquake

3-1. Zao volcano

The first volcanic tremor at Zao volcano was detected by the Japan Meteorological Agency on January

22, 2013, about one year and ten months after the 2011 Tohoku-Oki earthquake. Subsequently, volcanic earthquakes and tremors have been observed intermittently (Fig. 7) through the present. The peak times of volcanic earthquakes roughly correspond to the detection times of volcanic tremors. The interval between peaks was about two to three months until October 2013; subsequently, large peaks were observed in August 2014 and in April and June 2015. Afterward, no obvious peaks were seen, but volcanic tremors have been observed intermittently. Long-period shallow earthquakes have been detected beneath Zao since January 2013 (Yamamoto *et al.* 2014). Further, Yamamoto *et al.* (2014) reported that the number of low-frequency earthquakes has increased since about one year before the volcanic tremors were first detected. Other precursory phenomena have been observed including a slight inflation of the summit area from August 2014, an increase in underground temperature shown by a total magnetic force survey, and the appearance of white coloration in lake water caused by an infusion of volcanic gas.

In April 2015, there were about 30 volcanic earthquakes over four consecutive days. The Meteorological Agency announced a volcanic warning in the vicinity of the crater on April 13, which was withdrawn on June 16.

The hypocenter distribution maps of JMA (2016b) for volcanic earthquakes and tremors and for deep low-frequency earthquakes are shown in Fig. 8a. The Vp/Vs structure beneath Zao volcano (Okada *et al.*, 2015) is shown in Fig. 8b. The shallow hypocenters are plotted mostly within ~3 km in depth below sea level, whereas deep hypocenters are widely distributed between depths

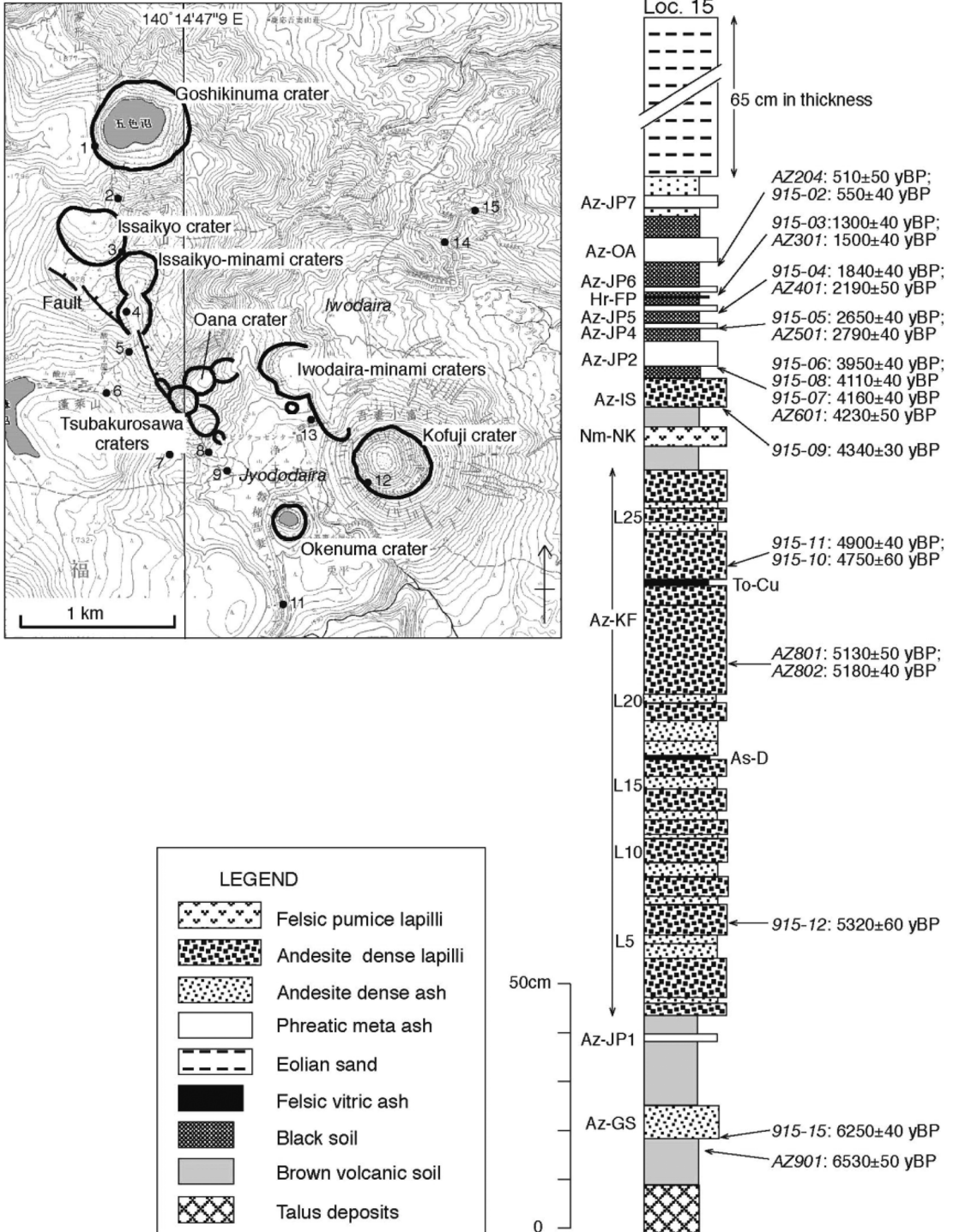


Fig. 5. Localities of craters and columnar section of the representative outcrop after Yamamoto (2005).

of ~20 km to 37 km. Some of the shallow earthquakes are 5–6 km deep. The deep earthquakes formed two clusters. One is from 20 km to 28 km and the other is from 28 km to 37 km depth. Okada *et al.* (2015) reported that in northeast Japan, shallow earthquake activity occurred in areas above the lower crust of high Vp/Vs.

The high Vp/Vs is related to the presence of melt. The deeper earthquakes in areas of high Vp/Vs were probably caused by migration of over-pressurized fluid.

3-2. Azuma volcano

The time sequence of volcanic earthquakes and tremors reported by JMA (2016c) is shown in Fig. 9.

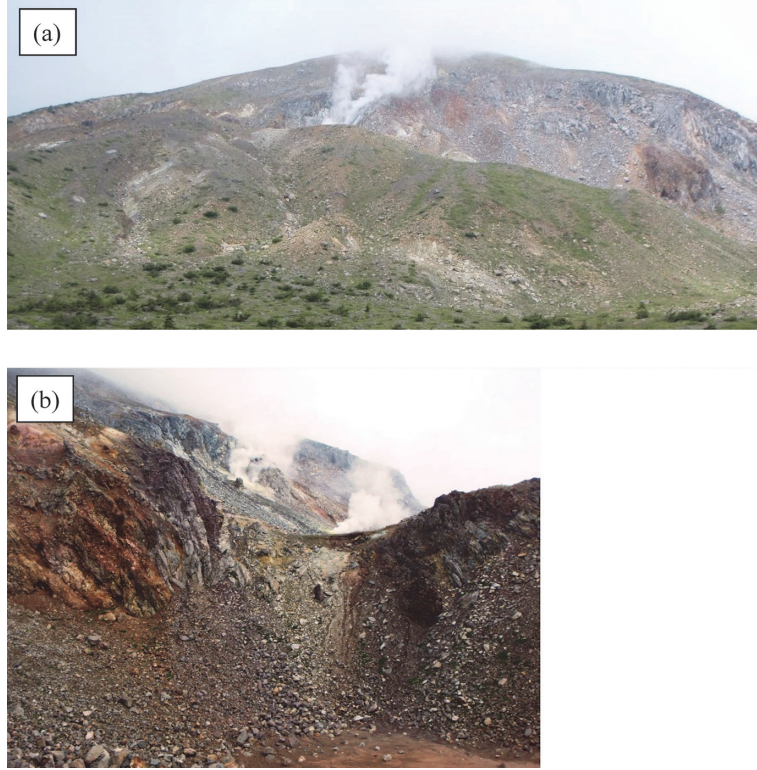


Fig. 6. Photographs of Oana crater emitting volcanic fumaroles. These images were captured (a) west and (b) south of the crater.

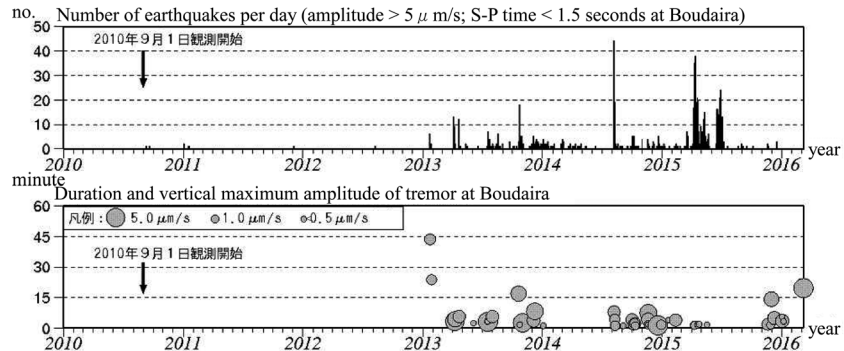


Fig. 7. Time sequence of volcanic earthquakes and tremors in Zao volcano from September 1, 2010 to March 7, 2016 (JMA, 2016a).

From 2001 to 2009, the intervals between peaks in volcanic earthquakes were about two to three years with or without tremors. Afterward, the tremors occurred with approximately 18-month intervals, and the periodicity of the peaks of volcanic earthquakes is unclear.

According to JMA (2016c), fumarolic activity at Oana crater has remained at relatively high levels and has intensified since November 11, 2008, and the geo-thermal area of the summit has widened since 2013. A slight deformation of the summit area occurred in July

2014, and an intense increase in underground temperature in October 2014 shown by the total magnetic force survey has also been observed.

The number of volcanic earthquakes has increased since October 2014, and a volcanic tremor was observed on December 12, 2014. At that time, the hazard status was increased to Alert Level 2 (JMA, 2014).

Hypocenter distribution maps for volcanic earthquakes and tremors and for deep low-frequency earthquakes beneath Azuma volcano of JMA (2016d) are

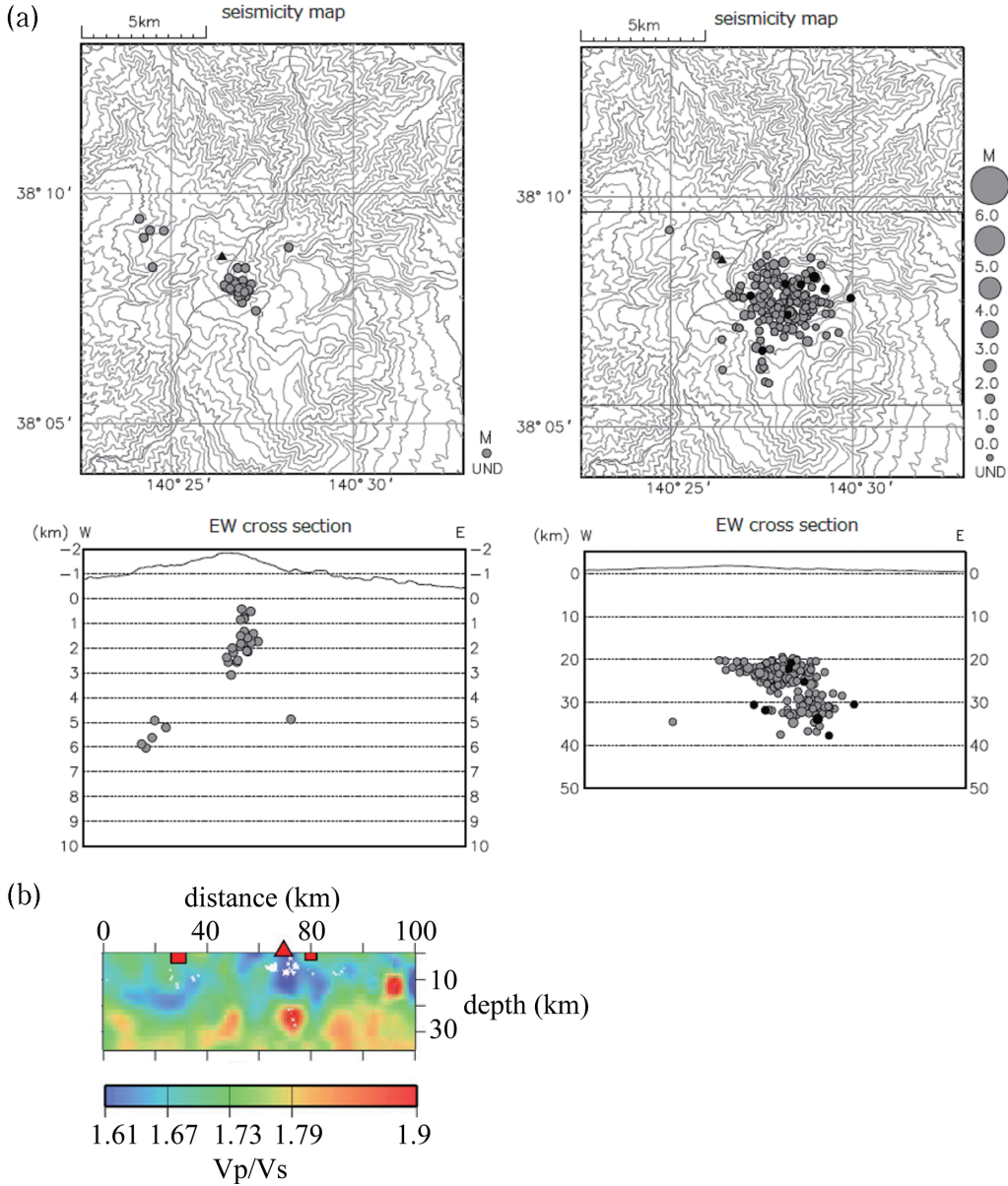


Fig. 8. (a) Hypocenter distribution maps of volcanic earthquakes and tremors occurring beneath Zao volcano from September 2010 to January 2015 and of deep long-period earthquakes occurring from September 1999 to January 2016 (JMA, 2016b). (b) V_p/V_s structure of the E-W vertical cross section through the center of Zao volcano (Okada *et al.*, 2015).

shown in Fig. 10 a. The V_p/V_s structure beneath Azuma volcano after Okada *et al.* (2015) is shown in Fig. 10b. Regarding the seismic tomography image, the same features and interpretations as those reported in Zao are applicable. The shallow hypocenters are plotted mostly within ~1 km in depth below sea level, whereas deep ones are widely distributed from about 23 to 37 km in depth.

4. Petrologic features of magmas from recent eruptions of Zao and Azuma volcanoes

Many petrologic studies show that shallow magma chambers beneath active volcanoes can survive for several tens of thousands of years as mush chambers (*e.g.*, Zellmer *et al.*, 2005). Changes in chamber characteristics, including composition, crystallinity, and temperature, occur through repeated infusions of hotter magma from depth. These infusions can trigger eruptions; thus, revealing the history of changes in magma chamber characteristics, and their relationship to the

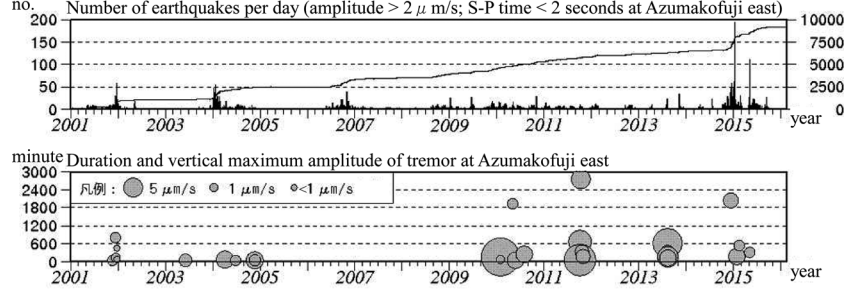


Fig. 9. Time sequence of volcanic earthquakes and tremors in Azuma volcano from January 1, 2001 to February 16, 2016 (JMA, 2016c).

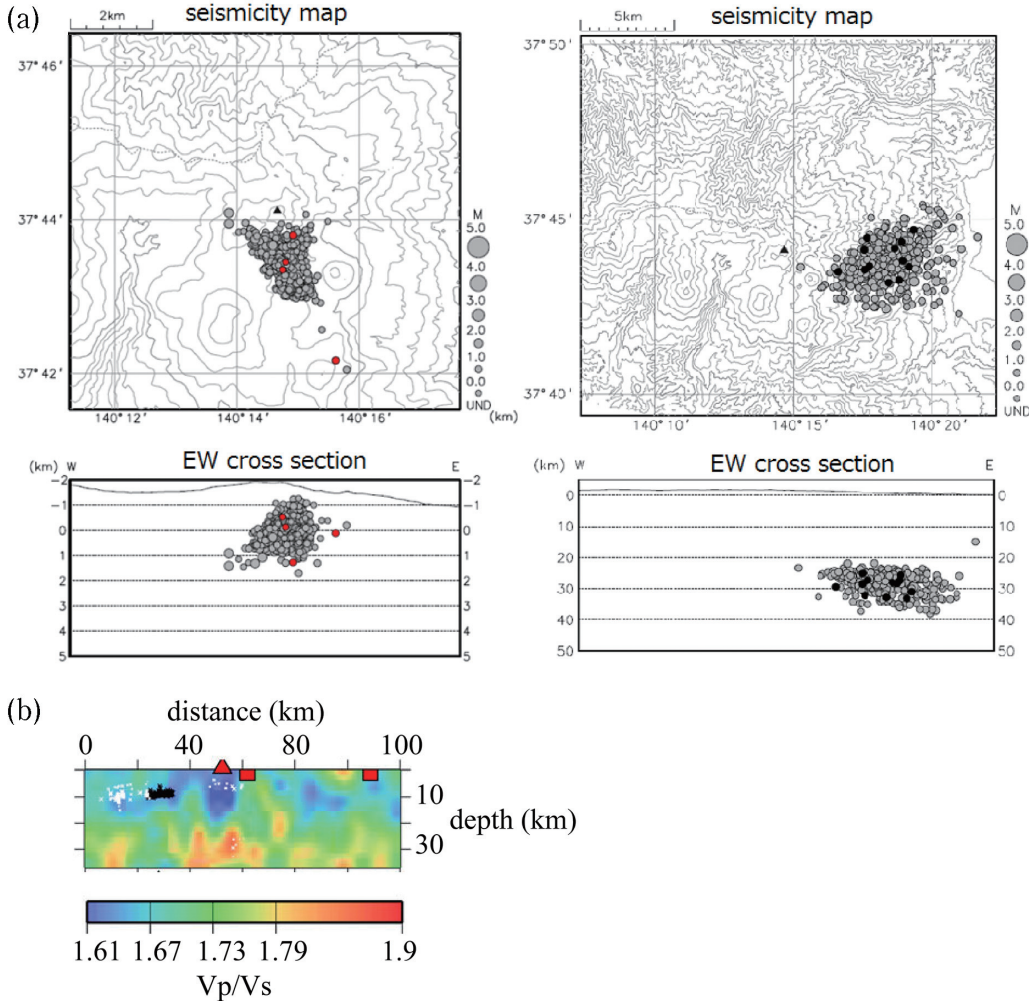


Fig. 10. (a) Hypocenter distribution maps for volcanic earthquakes and tremors and for deep long-period earthquakes beneath Azuma volcano from August 2003 to January 2016 (JMA, 2016d). (b) V_p/V_s structure of the E-W vertical cross section through the center of Azuma volcano (Okada *et al.*, 2015).

timing of eruptions is crucial. Therefore, we examined the petrologic characteristics of the chambers of recent magmatic eruptions of Zao and Azuma volcanoes.

4-1. Zao volcano

As described in Section 2-1, the youngest stage is

sub-divided into three phases. All of the eruption products of the youngest stage are mixed basaltic andesite to andesite and contain plagioclase, orthopyroxenes (opx), and clinopyroxenes (cpx) with or without olivine phenocrysts (Sakayori, 1991). The total volume of

Table 1. Estimated end-member magma compositions and chemical compositions of representative phenocrysts of Goshikidake pyroclastic rocks.

	SiO ₂	TiO ₂	Al ₂ O ₃	FeO ^t	Fe ₂ O ₃ ^t	MnO	MgO	CaO	Na ₂ O	K ₂ O	NiO	P ₂ O ₅	total
mafic end-member magma	50.50	0.65	16.80	12.00	—	0.19	7.60	11.02	1.89	0.09	—	0.12	100.86
felsic end-member magma	60.00	1.04	17.18	6.72	—	0.19	2.82	7.06	3.13	1.55	—	0.15	99.84
olv (form mafic magma)	39.84	—	—	17.28	—	0.37	43.74	0.16	—	—	0.14	—	101.52 Fo ₈₂
plg (from mafic magma)	47.20	—	33.21	—	0.80	—	0.07	17.87	1.10	0.03	—	—	100.29 An ₉₀
cpx (form felsic magma)	52.36	0.63	1.82	12.61	—	0.29	14.06	18.93	0.25	—	—	—	100.95 Mg#=67
opx (from felsic magma)	53.10	0.32	1.04	21.04	—	0.50	22.51	1.79	0.03	—	—	—	100.33 Mg#=66
plg (from felsic magma)	53.65	—	29.06	—	0.86	—	0.10	13.14	3.81	0.15	—	—	100.77 An ₆₅

olv, olivine; plg, plagioclase, cpx, clinopyroxene; opx, orthopyroxene; FeO^t, total iron calculated as FeO; Fe₂O₃^t, total iron calculated as Fe₂O₃

Analytical methods are after Ban *et al.* (2008)

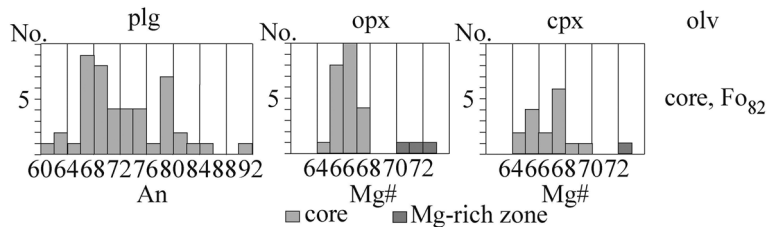


Fig. 11. Frequency histograms of plagioclase, opx, cpx, and olivine phenocrysts of the representative sample of Goshikidake pyroclastic rocks.

phenocrysts is about 25 to 30 %. All rocks have characteristics indicating magma mixing, such as dissolution textures in phenocrysts. The whole-rock compositions differ slightly among the three phases (Ban *et al.*, 2008). Here, we examine the petrologic features of the shallow magma chamber of the Goshikidake pyroclastic rocks phase, ~2 ka to the present, at Zao volcano. The chemical compositions of the phenocrysts from a representative sample are shown in Table 1 and Fig. 11.

On the basis of the chemical compositions, the phenocryst cores can be divided into three groups: An-rich plagioclase+olivine derived from the mafic magma, An- or Mg-medium plagioclase + pyroxenes from the mixed magma, and An- or Mg-poor plagioclase + pyroxenes from the felsic magma. In addition, some pyroxenes with Mg-poor cores have Mg-rich zones of ~30 µm in width in the rim parts (Fig. 11).

The felsic magma is in a shallow chamber, which was infused by the mafic magma rising from below; the erupted magma was formed by the mixing of these two magmas. Using a two-pyroxene thermometer (Brey and Köhler, 1990), we deduced the magmatic temperature from felsic magma-derived opx and cpx compositions to be approximately 955–970°C.

To estimate compositions of mafic and felsic end-members, we used key variation diagrams as follows.

In the K₂O-SiO₂ diagram (Fig. 12), the extension of the mixing trend by Goshikidake pyroclastic rock samples intercepts the SiO₂ axis at about 50.5 wt.%. In the Cr-SiO₂ diagram (Fig. 12), the extension of the mixing trend intercepts the SiO₂ axis at about 60 wt.%. Thus, we consider the SiO₂ contents of mafic and felsic magmas to be 50.5 wt.% and 60 wt.%, respectively. The compositions of the other elements in mafic and felsic magmas, listed in Table 1, were estimated from silica variation diagrams (Ban *et al.*, 2008).

Using the rhyolite-MELTS model (Gualda *et al.*, 2012) and estimated whole-rock compositions, we examined the ranges of pressure and water content of felsic magma to satisfy phenocrystic modal and chemical data. We note that the crystallinity of felsic magma was estimated to be ~40 % based on phenocrystic mode and mixing ratio. When the temperature is 955–970°C, plagioclase (An_{60–61})+opx (Mg#=65–66)+cpx (Mg#=66–68) precipitate under 1.3–1.5 kb and 1.7–1.8 % H₂O. Following Ban *et al.* (2008), an NNO buffer was assumed in this case. We attempted to determine the ranges for mafic magma using the same method. However, we could not establish the conditions under which Fo₈₂ olivine and An-rich plagioclase co-precipitated. It is probable that mafic magma, in which Fo-rich olivine was the only liquidus phase, differentiated to precipitate

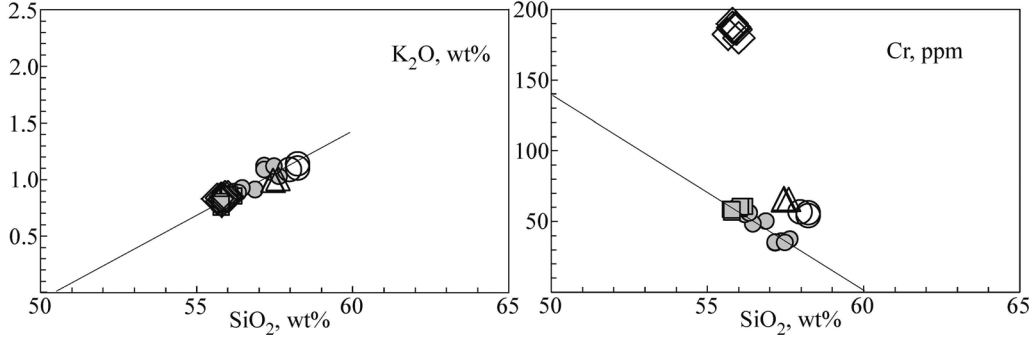


Fig. 12. K_2O and $\text{Cr}-\text{SiO}_2$ diagrams of Goshikidake pyroclastic rocks. Filled circles represent Goshikidake pyroclastic rocks; open symbols show Umanose agglutinate; and filled squares represent Komakusadaira pyroclastic rocks. Data are from Ban *et al.* (2008).

Table 2. Estimated end-member magma compositions and chemical compositions of representative phenocrysts of the Oana unit.

	SiO_2	TiO_2	Al_2O_3	FeO^t	Fe_2O_3^t	MnO	MgO	CaO	Na_2O	K_2O	NiO	P_2O_5	total
mafic end-member magma	50.00	0.81	17.50	11.00	—	0.19	8.71	10.90	1.82	0.15	—	0.11	101.18
felsic end-member magma	65.50	0.63	14.90	5.25	—	0.10	2.56	5.65	3.02	2.23	—	0.07	99.91
olv (form mafic magma)	39.59	—	—	15.98	—	0.26	45.69	0.22	—	—	0.13	—	101.87 Fo_{84}
plg (from mafic magma)	46.07	—	33.80	—	0.67	—	0.02	17.95	1.27	0.00	—	—	99.78 An_{89}
cpx (from felsic magma)	51.83	0.36	1.32	11.83	—	0.42	14.15	20.11	0.24	—	—	—	100.26 $\text{Mg\#}=68$
opx (from felsic magma)	52.52	0.19	0.77	23.55	—	0.63	21.68	1.47	0.06	—	—	—	100.87 $\text{Mg\#}=62$
plg (from felsic magma)	53.91	—	28.54	—	0.65	—	0.05	12.13	4.60	0.25	—	—	100.13 An_{58}

olv, olivine; plg, plagioclase, cpx, clinopyroxene; opx, orthopyroxene; FeO^t , total iron calculated as FeO ; Fe_2O_3^t , total iron calculated as Fe_2O_3

Analytical methods are after Ban *et al.* (2008)

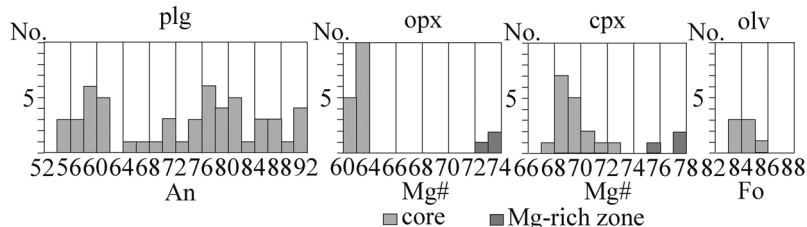


Fig. 13. Frequency histograms of plagioclase, opx, cpx, and olivine phenocrysts of the representative sample of the Oana unit.

plagioclase when Fo-rich olivine was no longer in the liquidus phase and further ascended to infuse into the shallow felsic chamber. We note the mafic magmas can precipitate Fo-rich olivine at $>$ about 1.5 kb, which is higher than the pressure condition of the felsic chamber.

4-2. Azuma volcano

As described in Section 2-2, five magmatic eruption phases are recognized in the youngest activity. The rocks are mainly andesite, having mixed rock characteristics such as mafic inclusions and dissolution textures in phenocrysts. These rocks have plagioclase, opx, cpx, and olivine phenocrysts. The total volume of phenocrysts is about 25 to 35 %. The whole-rock compositions differ slightly among the phases (Ban *et al.*, 2013).

Here, we examine petrologic features of the shallow magma chamber of the youngest phase (Oana unit of AD 1331). The chemical compositions of phenocrysts in a representative sample are presented in Table 2 and Fig. 13.

As in the case of Zao Goshikidake, phenocryst cores can be divided into three groups: mafic magma-derived An-rich plagioclase+olivine, mixed magma-derived An- or Mg-medium plagioclase+pyroxenes, and felsic magma-derived An- or Mg-poor plagioclase+pyroxenes. In addition, some pyroxenes with Mg-poor cores have Mg-rich zones \sim 30 μm in width in rim parts. The magmatic temperature deduced by felsic magma-derived opx and cpx compositions using Brey and Köhler (1990) is about

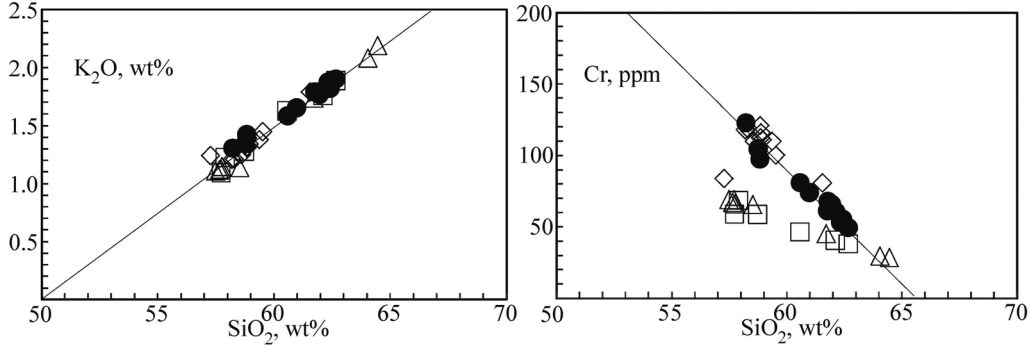


Fig. 14. K_2O and $\text{Cr}-\text{SiO}_2$ diagrams of the Oana unit. Filled circle, open triangle, open square, and open diamond represent Oana, Issaikyo, Kofuji, and Goshikinuma units. Data are from Ban *et al.* (2013).

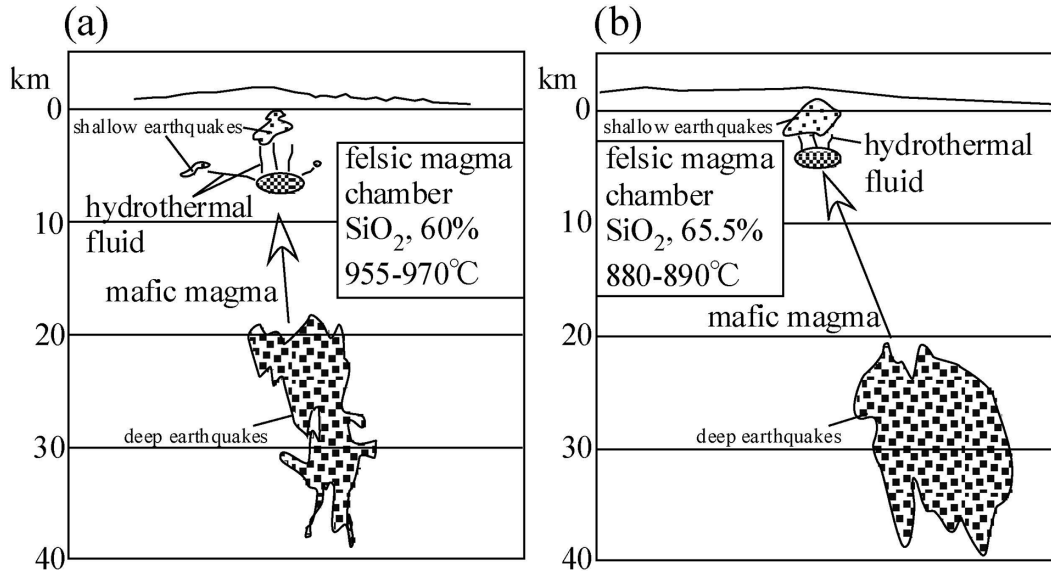


Fig. 15. Schematic diagram of magma feeding systems of (a) Zao and (b) Azuma volcanoes. Areas of deep and shallow hypocenters are from JMA (2016b, d).

$880-890^\circ\text{C}$.

As in the case of Zao Goshikidake, we used key variation diagrams to estimate compositions of mafic and felsic end-members as follows. The extension of the mixing trend by the Oana unit samples intercepts the SiO_2 axis at ~ 50 wt.% in the $\text{K}_2\text{O}-\text{SiO}_2$ diagram and at ~ 65.5 wt.% in the $\text{Cr}-\text{SiO}_2$ diagram (Fig. 14). Therefore, we consider the SiO_2 content of mafic and felsic magmas to be 50 wt.% and 65.5 wt.%, respectively. The compositions of other elements in mafic and felsic magmas, listed in Table 2, were estimated from the silica variation diagrams (Ban *et al.*, 2013).

Using the same method as that for Zao Goshikidake, we examined the ranges of pressure and water content of felsic magma. We note that the crystallinity of felsic magma was estimated to be $\sim 50\%$ based on pheno-

crystic mode and mixing ratio. When the temperature is $880-890^\circ\text{C}$, plagioclase (An_{58}) + opx ($\text{Mg\#} = 61-63$) + cpx ($\text{Mg\#} = 67-70$) precipitate under 0.8–1.2 kb and 2.75–3.25 % H_2O . An NNO buffer was also assumed. In terms of mafic magma, $\text{Fo}_{\text{ca},83}$ olivine and An-rich plagioclase co-precipitate at < 1.6 kb and ~ 1.25 wt.% H_2O .

5. Magma feeding system of recent eruptions of Zao and Azuma volcanoes

A schematic diagram of magma feeding systems is presented in Fig. 15. The basic framework of the magma feeding system is common for recent magmatic eruptions at Zao and Azuma. Mafic magmas from depth were infused into the shallower felsic magma chamber, which triggered eruptions; this process has been reported for many calc-alkaline volcanoes (*e.g.*, Pallister *et al.*, 1992;

Tomiya *et al.*, 2013). However, many differences were observed in the characteristics of mafic and felsic magmas. The mafic magma of Zao is slightly more differentiated than that of Azuma, and felsic magma of Zao has a slightly lower SiO₂ content than that of Azuma. As a result, felsic magma from Zao has higher temperature and pressure and lower crystallinity and water content than that from Azuma.

A comparison of the results of petrological studies with the hypocenter distribution (JMA, 2016b, d) and the seismic tomography image (Okada *et al.*, 2015) reveal important information. First, the estimated felsic chambers are located deeper than the shallow earthquakes including the volcanic tremor with the exception of several in Zao volcano. Shallow long-period earthquakes in Zao can be explained by oscillations of an open crack at ~2 km in depth that was filled with hydrothermal fluid, as revealed by a seismological analysis (Yamamoto *et al.*, 2014). These factors suggest that the shallow volcanic tremors were caused by activity related to the release of hydrothermal fluid from felsic magma. The other shallow earthquakes would be also related to the activity of hydrothermal fluid. Some scattering of hypocenters reflect various pathways of fluid from the chamber. Second, the depths of both shallow earthquakes and felsic magmas are greater in Zao than in Azuma, which reflects differences in felsic magma characteristics, crustal structure, or both. Third, no shallow magma chambers were detected with tomography (*e.g.*, Vp/Vs). It is probable that the shallow chambers are crystal-rich and may be small, and thus were difficult to detect with the tomographic survey. Fourth, potential candidates as sources of mafic magmas are high Vp/Vs and deep earthquake areas. The existence of melt in the area was reported by Okada *et al.* (2015), who argued that migration of over-pressurized fluids from this area promotes the occurrence of earthquakes because the seismic low-velocity area corresponds to an area containing over-pressurized fluids. As described above, recent eruptions of Zao and Azuma volcanoes were triggered by the injection of mafic magma into a shallow chamber. Therefore, it is crucial to detect melt movement from the seismic low-velocity area to the estimated shallow chambers in each volcano in forecasting future eruptions.

Acknowledgements

The authors would like to thank Professors E.

Takahashi and K. Kurita, who enabled publication of this article. Constructive comments from reviewers were very useful for revising the manuscript. Drs. T. Oikawa, S. Yamasaki, H. Yagi, M. Nakagawa, S. Hayashi, T. Ohba, A. Fujinawa, S. Miura, T. Nishimura, A. Goto, M. Yamamoto, M. Ichiki, N. Tsuchiya, and K. Nogami offered valuable advice. K. Maki, Y. Kawaharada, T. Nagaoka, K. Mizugishi, T. Takahashi, T. Waga, K. Ohta, and S. Abe of JMA provided important information about recent Zao volcano activity. The prefectures of Yamagata and Miyagi provided permission to survey national parks. In addition, the authors would like to extend sincere thanks to all who assisted in this research. This work was financially supported in part by a Grant-in-Aid for Scientific Research from the Japan Society for the Promotion of Science to M. Ban (Nos. 21510186 and 26400509) and by the Earthquake Research Institute, University of Tokyo cooperative research program.

References

- Amma-Miyasaka, M. and M. Nakagawa, 2003, Evolution of deeper basaltic and shallower andesitic magmas during the AD 1649–193 eruptions of Miyake-jima volcano, Izu-Mariana arc : inferences from temporal variation of mineral compositions in crystalclots, *J. Petrol.*, **44**, 2113–2138.
- Ban, M., 2013, Zao Volcano, *J. Geol. Soc. Japan*, **119**, Supplement, S120–S133 (in Japanese with English abstract).
- Ban, M., H. Sagawa, K. Miura, and S. Hirotani, 2008, Evidence for short-lived stratified magma chamber : petrology of Z-To tephra layer (~5.8 ka) at Zao volcano, NE Japan, in “*Dynamics of Crustal Magma Transfer, Storage, and Differentiation Integrating Geochemical and Geophysical Constraints*”, edited by Zellmer, G. and C. Annen, Geol. Soc. London, Special Publication, **304**, pp. 149–168.
- Ban, M., Matsui, R., Yamamoto, T., Iwata, N., Fujinawa, A., Nakashima, K., 2013, Petrologic characteristics of the newest stage in Azuma volcano group, Northeast Japan. *Int. J. Erup. Histo. Informa.*, **1**, 1–10.
- Ban, M., T. Oikawa, and S. Yamasaki, 2015, Geological map of Zao volcano, *Geological Map of Volcanoes*, no. 18, Geological Survey of Japan, AIST (in Japanese with English abstract).
- Brey, G. and T. Köhler, 1990, Geobarometry in four phase lherzolites II. New thermobarometers, and practical assessment of existing thermobarometers. *J. Petrol.*, **31**, 1353–1378.
- Fujinawa, A. and T. Kamoshida, 1990, Azuma volcano, in “*Volcanoes in the Tohoku Region: Field Guide of Japanese Volcano 4*”, edited by Takahashi, M. and T. Kobayashi, Tsukijishokan, Tokyo, pp. 89–104 (in Japanese).
- Garcia, M.O., A.J. Pietruszka, J.M. Rhodes, and K. Swanson, 2000, Magmatic processes during the prolonged Pu'u'O'o eruption of Kilauea Volcano, Hawaii, *J. Petrol.*, **41**, 967–990.
- Geological Survey of Japan, AIST, 2016, Azumayama, Active volcanoes of Japan, https://gbank.gsj.jp/volcano/Quat_

- Vol/volcano_data/D62.html (in Japanese).
- Gualda, G. A. R., M. S. Ghiorso, R. V. Lemons, and T. L. Carley, 2012, Rhyolite-MELTS : a modified calibration of MELTS optimized for silica-rich, fluid-bearing magmatic systems, *J. Petrol.*, **53**, 875–890.
- JMA, 2014, Volcanic Activity Report (Azumayama) (12th December 2014), http://www.data.jma.go.jp/svd/vois/data/tokyo/STOCK/monthly_v-act_doc/sendai/14m12/20141212_213.pdf (in Japanese).
- JMA, 2016a, Volcanic Activity Report (Zaozan) (7th March 2016), http://www.data.jma.go.jp/svd/vois/data/tokyo/STOCK/monthly_v-act_doc/sendai/16m03/20160307_212.pdf (in Japanese).
- JMA, 2016b, Zaozan. In: 134th Meeting Materials (2–6) of the Coordinating Committee for Earthquake Prediction, 55–72, http://www.data.jma.go.jp/svd/vois/data/tokyo/STOCK/kaisetsu/CCPVE/shiryo/134/134_02-6.pdf (in Japanese).
- JMA, 2016c, Volcanic Activity Report (Azumayama) (17th February 2016), http://www.data.jma.go.jp/svd/vois/data/tokyo/STOCK/monthly_v-act_doc/sendai/16m02/20160217_213.pdf (in Japanese).
- JMA, 2016d, Azumayama. In: 134th Meeting Materials (2–5) of the Coordinating Committee for Earthquake Prediction, 43–59, http://www.data.jma.go.jp/svd/vois/data/tokyo/STOCK/kaisetsu/CCPVE/shiryo/134/134_02-5.pdf (in Japanese).
- Kawano, Y., K. Yagi, and K. Aoki, 1961, Petrography and petrochemistry of the volcanic rocks of Quaternary volcanoes of northeastern Japan, *Sci. Rep. Tohoku Univ., Ser. III*, **7**, 1–46.
- Kochibe, T. (1896) Summary Report of Research on Eruptions of Zao Volcano. *J. Geography*, **8**, 183–189, 239–244, 285–288 (in Japanese).
- Kuno, H., 1962, Japan, Taiwan and Marianas, in "Catalog of Active Volcanoes of the World and Solfatara Fields, Rome", edited by IAVCEI, **11**, pp. 1–332.
- Miura, K., M. Ban, T. Ohba, and A. Fujinawa, 2012, Sequence of the 1895 eruption of the Zao volcano, Tohoku Japan, *J. Volcanol. Geotherm. Res.*, **247–248**, 139–157.
- NEDO, 1991, Geological and geothermal survey maps of Azuma district. 80 p (in Japanese).
- Nicotra, E. and M. Viccaro, 2012, Transient uprise of gas and gas-rich magma batches fed the pulsating behavior of the 2006 eruptive episodes at Mt. Etna volcano, *J. Volcanol. Geotherm. Res.*, **227–228**, 102–118.
- Oba, Y. and T. Konta, 1989, Geology and petrology of Central Zao Volcano, Yamagata Prefecture. *Bull. Yamagata Univ. Nat. Sci.*, **12**, 199–210 (in Japanese with English abstract).
- Oikawa, T. and M. Ban, 2013, History and style of the historical age eruption of Zao Volcano, NE Japan, Abstracts of the 120th Annual Meeting of the Geological Society of Japan, p. 44 (in Japanese).
- Okada, T., T. Matsuzawa, N. Umino, K. Yoshida, A. Hasegawa, H. Takahashi, T. Yamada, M. Kosuga, T. Takeda, A. Kato, T. Igarashi, K. Obara, S. Sasaki, T. Iidaka, T. Iwasaki, N. Hirata, N. Tsumura, Y. Yamanaka, T. Terakawa, H. Nakamichi, T. Okuda, S. Horikawa, H. Katao, T. Miura, A. Kubo, T. Matsushima, K. Goto, and H. Miyamachi, 2015, Hypocenter migration and crustal seismic velocity distribution observed for the inland earthquake swarms induced by the 2011 Tohoku-Oki earthquake in NE Japan : implications for crustal fluid distribution and crustal permeability, *Geofluids*, **15**, 293–309.
- Pallister, J.S., R.P. Hoblitt, and A.G. Reyes, 1992, A basalt trigger for the 1991 eruptions of Pinatubo volcano? *Nature*, **356**, 426–428.
- Sakayori, A., 1991, Magmatic evolution of Zao volcano, Northeast Japan, *Bull. Volcanol. Soc. Japan*, **36**, 79–92 (in Japanese with English abstract).
- Sakayori, A., 1992, Geology and petrology of Zao Volcano, *J. Mineral. Petrol. Econ. Geol.*, **87**, 433–444 (in Japanese with English abstract).
- Shamberger, P.J. and M.O. Garcia, 2007, Geochemical modeling of magma mixing and magma reservoir volumes during early episodes of Kīlauea Volcano's Pu'u 'Ō'ō eruption. *Bull. Volcanol.*, **69**, 345–352.
- Savov, I.P., J.F. Luhr, and C. Navarro-Ochoa, 2008, Petrology and geochemistry of lava and ash erupted from Volcán Colima, Mexico, during 1998–2005, *J. Volcanol. Geotherm. Res.*, **174**, 241–256.
- Takaoka, N., K. Konno, Y. Oba, and T. Konta, 1989, K-Ar datings of lavas from Zao Volcano, north-eastern Japan, *J. Geol. Soc. Japan*, **95**, 157–170 (in Japanese with English abstract).
- Tiba, T., 1961, Petrological study of Zao volcano, *J. Japan. Assoc. Mineral. Petrol. Econ. Geol.*, **46**, 74–81 (in Japanese with English abstract).
- Tomiya, A., I. Miyagi, G. Saito, N. Geshi, 2013, Short time scales of magma-mixing processes prior to the 2011 eruption of Shinmoedake volcano, Kirishima volcanic group, Japan, *Bull. Volcanol.*, **75**, 750–769.
- Yamamoto, T., 2005, Eruptive history of Azuma volcano, NE Japan, during last 7,000 years : Stratigraphy and magma plumbing system of the Azuma Jododaira products, *J. Geol. Soc. Japan*, **111**, 94–110 (in Japanese with English abstract).
- Yamamoto, M., S. Miura, M. Ichiki, and S. Hirahara, 2014, The shallow long-period earthquake activity and its generation mechanism in Zao volcano, Abstracts of 2014 Fall Meeting of Volcanol. Soc. Japan, p.53 (in Japanese).
- Zellmer, G.F., C. Annen, B.L.A. Charlier, R.M.M. George, S.P. Turner, and C.J. Hawkesworth, 2005, Magma evolution and ascent at volcanic arcs : Constraining petrogenetic processes through rates and chronologies, *J. Volcanol. Geotherm. Res.*, **140**, 171–191.

(Received May 19, 2016)

(Accepted January 26, 2017)

蔵王山、吾妻山の活動史と最近の噴火をもたらしたマグマ溜まり

伴 雅雄^{1)*}・武部義宜¹⁾・足立辰也¹⁾・松井るり子¹⁾・西 勇樹¹⁾

¹⁾ 山形大学理学部地球環境学科

要 旨

2011年3月11日に発生した東北地方太平洋沖地震の後、東北地方の幾つかの火山、特に震源に近い蔵王山と吾妻山では火山活動の活性化が見られる。本論では、両火山の噴火史と現況をレビューし、また最近の噴出物の岩石学的なデータに基づき、地下のマグマ供給系について検討した。

両火山共に約100万年の噴火の歴史がある。蔵王山の活動は、約100万年前の水中噴火で特徴づけられる活動、約50-4万年前の安山岩質中小規模火山の形成で特徴づけられる活動、約3.5万年前以降の玄武岩質安山岩～安山岩質マグマの爆発的噴火で特徴づけられる活動に大きく分けられる。約3.5万年前以降の活動はさらに、約3.5-1.3万年前、9-4千年前、約2千年前以降のフェーズに分けられ、このうち最後のフェーズで現在の火口湖御釜を胚胎する五色岳が形成された。噴火記録も多数あり、御釜からの最新の噴火活動は1894～97年である。吾妻山の活動は約120-80、80-60、60-40、40-30万年前と30万年前以降の5つに大きく分けられる。各時期に、多数の安山岩質中小規模成層火山が吾妻山全域に亘って形成された。30万年前以降の活動期の中でも現在に続く活動は、約7千年前に始まった東部の活動である。この間、約6.7、6.3、5.9～4.8千年前、4.3千年前と西暦1331年にマグマ噴火が発生した。水蒸気爆発も多数発生しており、最新のものは1977年に起こっている。

蔵王山では2013年1月に火山性微動が初めて観測された。一方吾妻山ではそれまでにも火山性微動は観測されていたが、2010年の1月から振幅の大きなものが観測され始めた。火山性地震の回数が、蔵王山では2014年

の4月に、吾妻山では12月に増加し、同時に火山性微動や山頂方面の膨張も観測されたため、噴火警報（火口周辺）の発令に至った。蔵王山では6月に解除されたが吾妻山では継続している。両火山共に、噴気活発化など他の兆候も認められている。

両火山の最近の主な噴出物は、中間カリウム・カルクアルカリ玄武岩質安山岩～安山岩で、汚濁帶、逆累帯構造を持つ斑晶や非平衡的斑晶組み合わせが認められる混合岩である。岩石学的な検討を行った結果、珪長質端成分は、蔵王山ではSiO₂量が約60%の安山岩で、温度・圧力・含水量条件は955-970°C, 1.3-1.5 kb, 1.7-1.8%, 吾妻山ではSiO₂量が約65.5%のデイサイトで、温度・圧力・含水量条件は880-890°C, 0.8-1.2 kb, 2.75-3.25%と推定された。苦鉄質端成分は両火山共に玄武岩である。蔵王の方が吾妻よりもやや分化した組成である。浅部（地下約4～6km程度）に位置する珪長質端成分マグマに深部由来の苦鉄質端成分マグマが注入・混合して噴出したと考えられる。

両火山共に、珪長質マグマは浅部火山性地震の震源位置よりもやや深所に存在していると考えられる。浅部火山性地震を引き起こしていると考えられる熱水は、この珪長質マグマ由来の可能性が高い。また、深部低周波地震は、その震源域が地震トモグラフィーによる高Vp/Vs域にあることから、メルトの移動によるものと考えられており、そのメルトが苦鉄質端成分マグマの起源である可能性が考えられる。

キーワード：蔵王山、吾妻山、活動史、2011年東北地方太平洋沖地震、マグマ供給系